Int. J. Electrochem. Sci., 5 (**2010**) 605 - 614

International Journal of
ELECTROCHEMICAL
SCIENCE
www.electrochemsci.org

Reduction of V^{4+} from V^{5+} using polymer as a surfactant for electrochemical applications

V S Reddy Channu[1], *Rudolf Holze*[1], *B. Rambabu* [2], *Rajamohan R. Kalluru*[3], *Quinton L. Williams*[3], *Chen Wen*[4]
[1] Institut für Chemie, AG Elektrochemie, Technische Universität Chemnitz,
D-09107 Chemnitz, Germany
[2] Department of Physics, Southern University and A&M College, Baton Rouge, LA 70813, USA
[3] Department of Physics, Atmospheric Sciences and Geoscience,
Jackson State University, JSU Box. 17660, 1400 J.R. Lynch Street, Jackson, MS 39217, USA
[4] Institute of Materials Science & Engineering, Wuhan University of Technology,
Wuhan , PR China
*E-mail: chinares02@gmail.com

Received: 26 April 2010 / *Accepted:* 15 May 2010 / *Published:* 30 May 2010

Vanadium dioxide nanowires and nanobelts were synthesized from vanadium pentoxide xerogel through a hydrothermal process. V^{5+} was reduced to V^{4+} by a polyblend of poly(vinyl pyrrolidone) (PVP) and poly(vinyl alcohol)(PVA), and by poly(vinyl alcohol)(PVA). Scanning electron microscopy (SEM) images confirm that polyblend (PVP+PVA) as a reducing agent resulted in nanowire morphology, PVA resulted in nanobelt morphology of vanadium dioxide. Thermal gravimetric analysis (TGA) curves exhibit weight gain in the temperature range 380 ℃ – 420 ℃ indicating oxidation of V^{4+}. X-ray diffraction results of heat treated nanobelts confirmed the oxidation of V^{4+} and the formation of vanadium pentoxide. Electrochemical studies show that the working electrode made of nanowires yields higher current density than the working electrode made of nanobelts.

Keywords: V_2O_5 xerogel, Nanomaterials, Reducing agent, Cyclic voltammogram

1. INTRODUCTION

In recent years, low-dimensional nanostructured materials, such as nanobelts, nanowires, nanotubes and nanorods have received significant attention because of their extraordinary properties [1,2]. On the other hand, the awareness of practical low-dimensional nanostructured materials depends not only on the quality of the size and dimensionality of the materials but also on their spatial direction and orientation. The development of realistic strategies in the fabrication of patterns of well-arranged nanocrystallities, particularly the arrangement of nanobelts, nanorods, nanowires and nanotubes will require significant study.

Among a number of known vanadium oxides, metastable oxides, designated as VO_2 (B), V_2O_3, V_6O_{13}, V_2O_5 and V_3O_7, were widely used in electrochemical devices as a cathode [3-7]. A number of polymorphs of vanadium dioxide are well known such as: VO_2(M), a monoclinically distorted rutile structure associated with a metal–insulator transition; VO_2(R) with the rutile structure; VO_2(A) with a tetragonal structure; and VO_2(B), which is isostructural with TiO_2(B) [8–10]. The polymer intercalated metal oxide nanomaterials [11-14] show high conductivity because of the enhanced surface area. Many studies have been conducted on polymer intercalated metal oxide thin films [15, 16] but only a few studies are available on polymer intercalated metal oxide nanopowders.

Using various techniques vanadium oxide nanostructures were successfully synthesized [1]. Recently we made an attempt on the bulk quantity synthesis and characterization of $H_2V_3O_8$ nanobelts using PEO, PEG[17], and VO_2(B) nanorods using PVP as a reducing agent and Li^+ as a template between vanadium oxide layers [3]. In this work, we describe the synthesis, structure, morphology and Li^+-extraction and intercalation of VO_2(B) nanowires and nanobelts using polyblend(PVP+PVA) and PVA as reducing agents from V_2O_5 xerogel through a simple hydrothermal synthesis.

2. EXPERIMENTAL PART

A brownish V_2O_5 xerogel was obtained through V_2O_5 melt quenching. The V_2O_5 powder (99.5%) was heated up to 800 ºC and kept at this temperature for 10 min; then quickly poured into distilled water. A red V_2O_5 xerogel was obtained after one week aging of the solution. For the preparation of vanadium dioxide nanomaterials, 20 ml of reducing agent solution (PVA and polyblend(PVP+PVP)) were added to 80 ml of V_2O_5 xerogel. The resulting mixture was transferred into an autoclave for hydrothermal reaction at 180˚C for 15 days. The final product of vanadium dioxide nanomaterials was then washed and dried at 100 ºC for 10 h.

Crystallographic information of the samples was obtained using an X-ray powder diffractometer (D8 Advance Brucker) equipped with graphite monochromatized Cu Kα radiation ($\lambda = 1.54187$ Å). Diffraction data were collected in the 2θ range 5° to 70˚. FTIR absorption spectra of the nanomaterials were measured using a Brucker IR spectrometer (4 cm^{-1} resolution) in the range 400 to 4000 cm^{-1}. The morphologies of the resulting products were characterized using a scanning electron microscope (SEM, JEOL JSM 6390). For the TGA measurements, a model TA 600 operating in dynamic mode (heating rate =10^{o}C/min) was employed. The electrochemical properties of the nanomaterials were investigated with a three-electrode cell with a platinum foil counter electrode and a silver (Ag) wire as a reference electrode. The working electrode, prepared by mixing 80 wt% of active material, 15 wt% of acetylene black and 5 wt% of polytetrafluoroethylene (PTFE), was coated on ITO glass (1.0 cm^2). A solution of 1 M lithium perchlorate (99.99%, Aldrich) in propylene carbonate (99.7 %, Aldrich) was used as the electrolyte after purification by recrystallization and distillation, respectively. Cyclic voltammetric (CV) measurements were carried out between the potential limits -1.0 V and +1.0 V versus a

Ag wire with a potentiostat/galvanostat (PRE 273). The CV curves were recorded at a scan rate of 10 mV/s.

3. RESULTS AND DISCUSSION

Figs. 1 and 2 show the XRD patterns of the VO_2(B) nanomaterials. All diffraction peaks can be indexed to the VO_2(B) monoclinic structure with lattice constants of a = 12.03 Å, b = 3.693 Å and c = 6.42 Å, and β = 106.6° (JCPDS # 31 -1438). No peaks of any other phases or impurities were observed, demonstrating that VO_2(B) nanomaterials with high purity could be obtained using the present synthetic process where (PVP+PVA) and PVA serve as surfactants as well as reducing agents. The peak separation is noticed clearly at 2θ =15°, 30° and 45° with increasing (PVP + PVA) composition. The products were in black color after the hydrothermal process, which indicates that V^{5+} cations were reduced to V^{4+} cations [3]. The (PVP+PVA) and PVA played a critical role in the formation of VO_2(B) nanowires and nanobelts during the hydrothermal process.

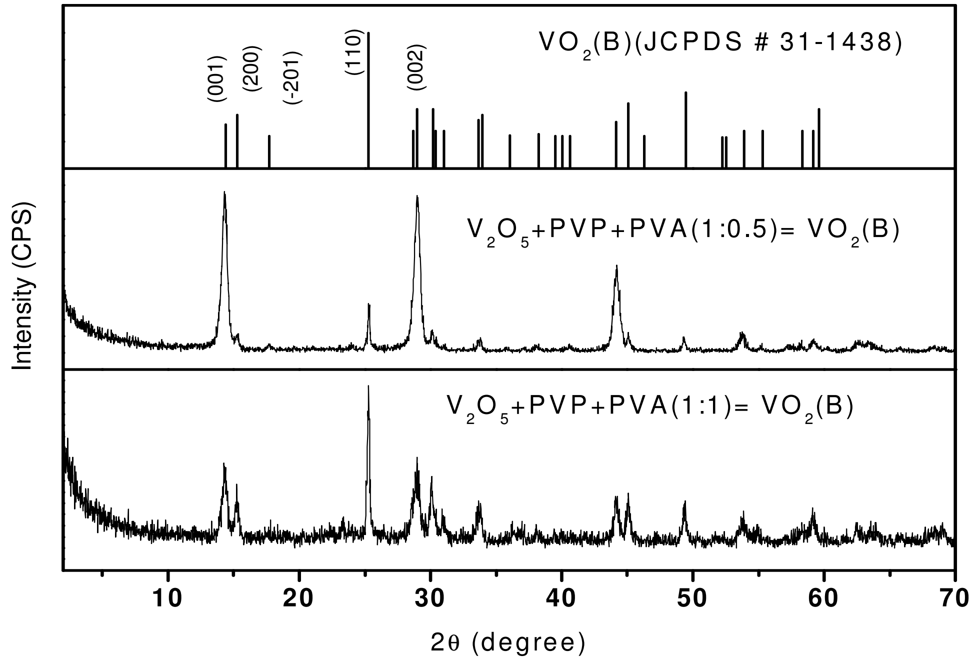

Figure 1. XRD patterns of reduced vanadium dioxide nanomaterials from V_2O_5 xerogel using PVP+PVA as a surfactant.

Fig. 3 shows the XRD patterns of the converted V_2O_5 nanobelts by heat-treatment of VO_2(B) nanobelts at 400 °C [4]. All the diffraction peaks can be indexed to the orthorhombic structure V_2O_5 with lattice constants of a = 11.516 Å, b = 3.5656 Å and c = 4.3727 Å (JCPDS # 00-041-1426).

The FTIR spectra of VO_2(B) nanowires are shown in Fig. 4. The bands between 1000 – 400 cm^{-1} can be assigned to various vibrations of V-O bonds. The broad band at 531 cm^{-1} can be assigned to the V-O-V octahedral bending modes. The band at 917 cm^{-1} can be associated with the stretching of short V=O bonds [18]. The weak band appears at 1011cm^{-1} due to initial disorder from VO_2 (B) octahedral arrangement. The broad absorption band at 3414 cm^{-1} is due to water in the xerogel [3].

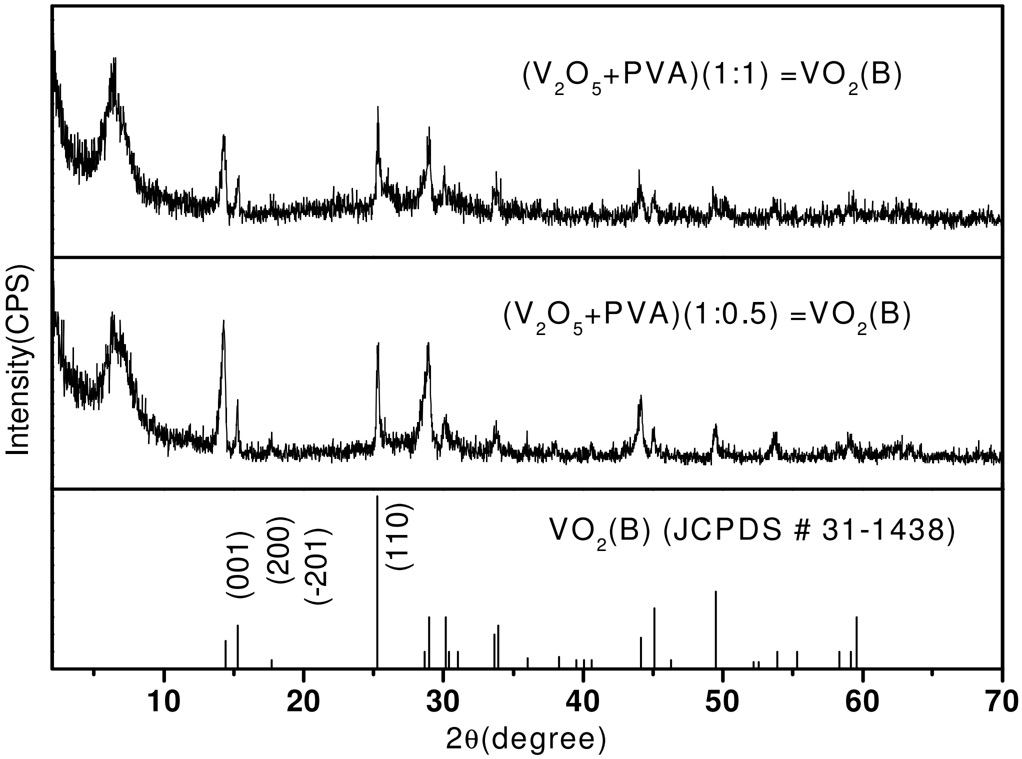

Figure 2. XRD patterns of reduced vanadium dioxide nanomaterials from V_2O_5 xerogel using PVA as a surfactant.

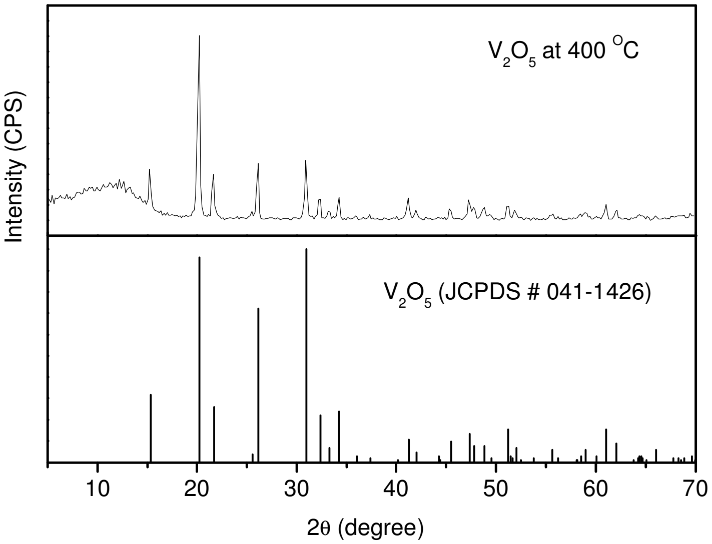

Figure 3. XRD patterns of V_2O_5 nanomaterials from vanadium dioxide (PVA as a surfactant).

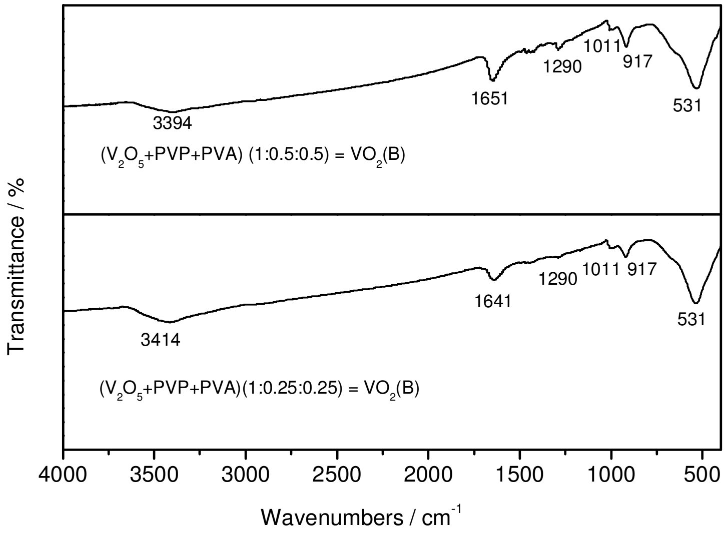

Figure 4. FTIR patterns of reduced vanadium dioxide nanomaterials from V_2O_5 xerogel using PVP+PVA as a surfactant.

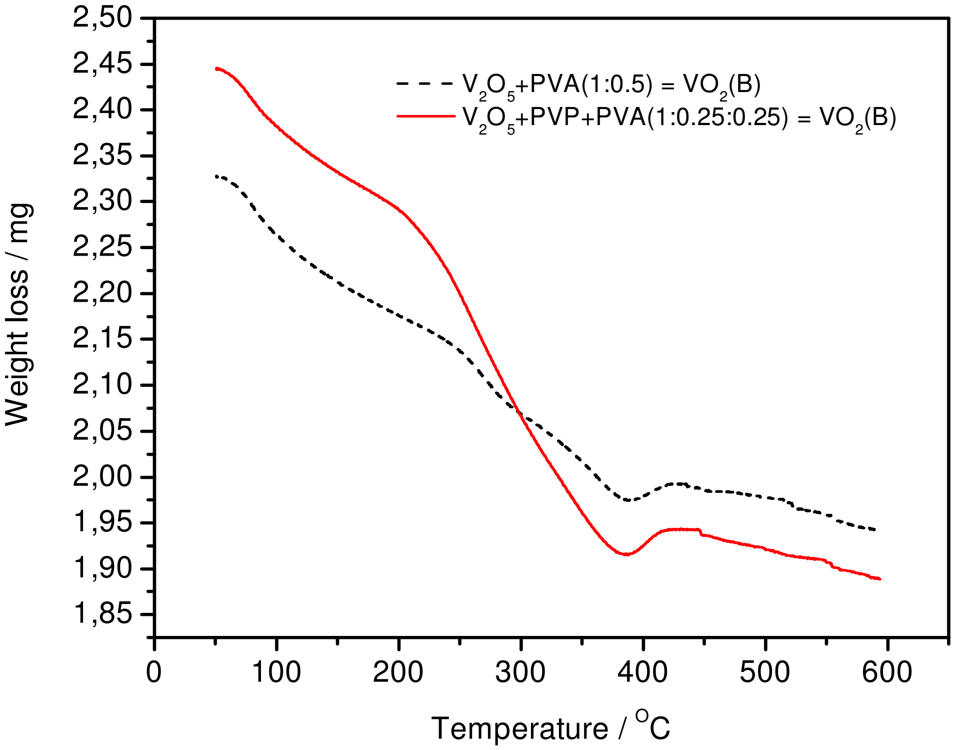

Figure 5. TGA curves of vanadium dioxide nanomaterials

The thermal gravimetric analysis (TGA) curves of VO_2 (B) nanowires and nanobelts are shown in Fig. 5. The first weight loss is 0.14 mg with (V_2O_5 + PVP + PVA) (1: 0.25 :0.25) → VO_2(B) nanowires in the temperature range 50 - 186 ℃, whereas the first weight loss is 0.175 mg with (V_2O_5 + PVA) (1: 0.5) → VO_2 (B) nanobelts in the range 50 - 230 ℃. This first weight loss can be attributed to evaporation of water from the layers of vanadium oxide xerogel. The second weight loss is 0.387 mg for nanowires in the temperature range 186 - 380 ℃ and 0.177 mg for nanobelts in the temperature range 230 - 380 ℃ due to decomposition of (PVP+PVA) and PVA trapped in the layers of vanadium oxide xerogel. The weight gain (0.02 mg) observed in the temperature range of 380 - 420 ℃ in both nanowires and nanobelts is due to the oxidation of V^{4+} yielding V_2O_5 [4,7]. These results were confirmed by the XRD patterns of nanobelt samples heat-treated at 400 ℃ (Fig. 3).

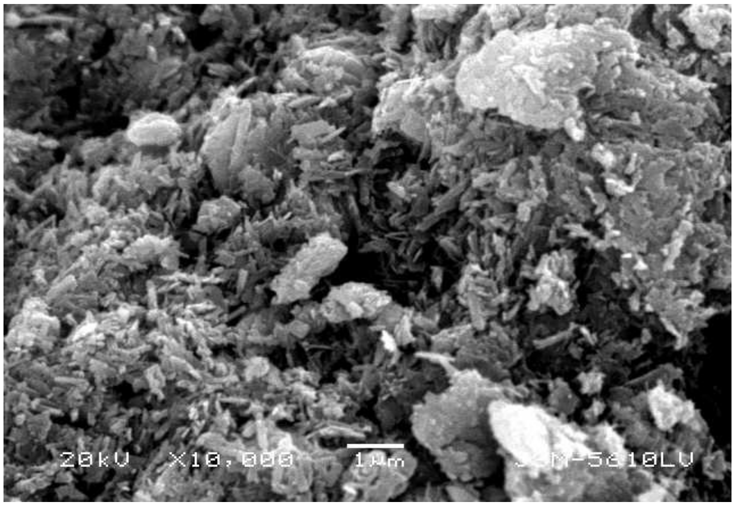

Figrue 6a. SEM photographs of reduced vanadium dioxide nanomaterials from V_2O_5 xerogel using 0. 5 M (PVP+PVA) as a surfactant.

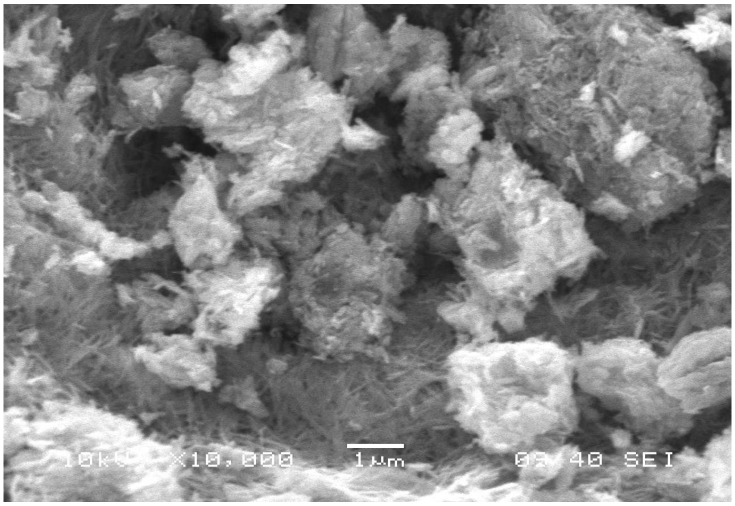

Figure 6b. SEM photographs of reduced vanadium dioxide nanomaterials from V_2O_5 xerogel using 1.0 M (PVP+PVA) as a surfactant.

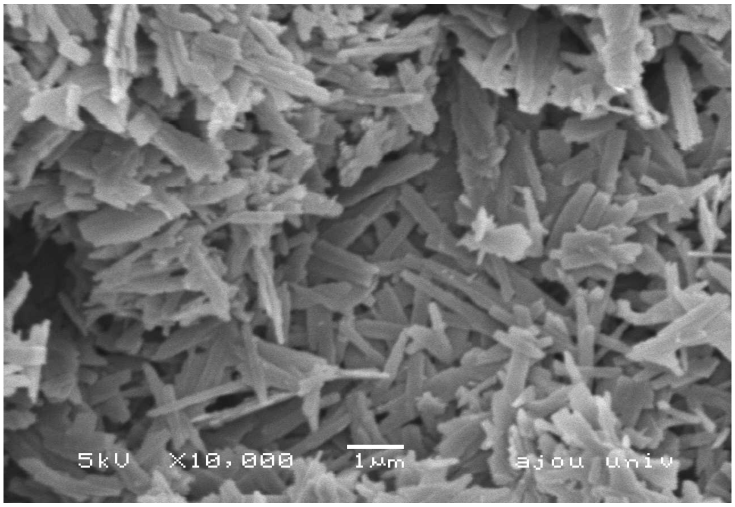

Figure 6c. SEM photographs of reduced vanadium dioxide nanomaterials from V_2O_5 xerogel using 0. 5 M PVA as a surfactant.

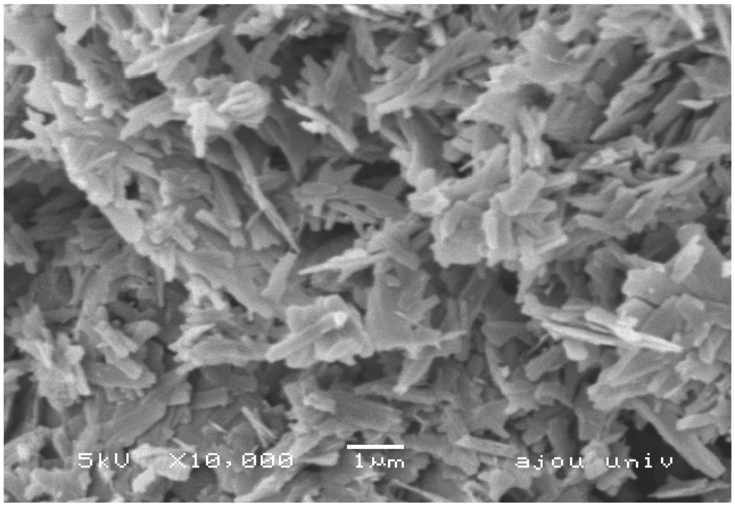

Figure 6d. SEM photographs of reduced vanadium dioxide nanomaterials from V_2O_5 xerogel using 1. 0 M PVA as a surfactant.

The surface morphology and size of VO_2 (B) nanowires and nanobelts are shown in Fig. 6. The SEM images of (V_2O_5 + PVP + PVA) → VO_2 (B) (Fig. 6a, 6b) show the homogenous phase of nanowires with uniform size 1 – 5 μm in length and about 100 nm in average diameter. The SEM photographs of (V_2O_5 + PVA) → VO_2 (B) (Fig. 6c, 6d) reveal the nanobelts' morphology size to be about several micrometers in length and about 200 nm in average width. Fig. 6e shows the SEM image of nanobelts that have been heat-treated at 400 °C. The nanobelts are maintaining the same morphology with increased dimensions, even after heat-treatment. This also clearly observed from XRD patterns of nanobelts heat-treated at 400 °C (Fig.3). In comparison, as the peak width of heat-treated nanobelts decreases, thus particle size increases [19].

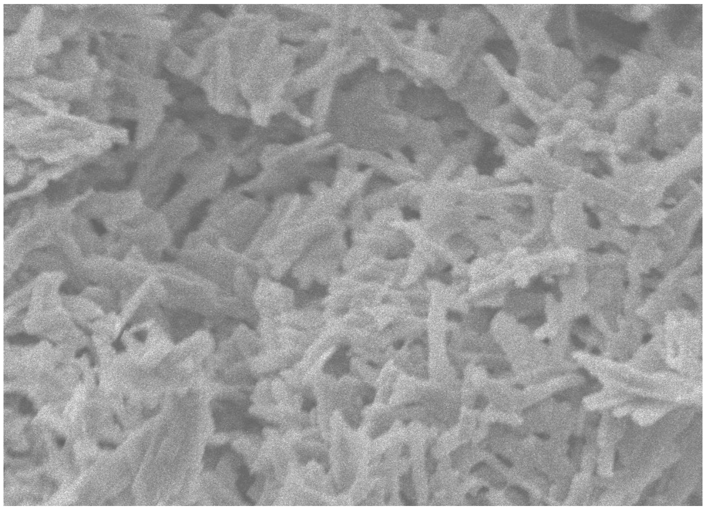

Figure 6e. SEM photographs of V_2O_5 nanomaterials from vanadium dioxide (using 0. 5 M PVA as a surfactant) at 400 ^{O}C.

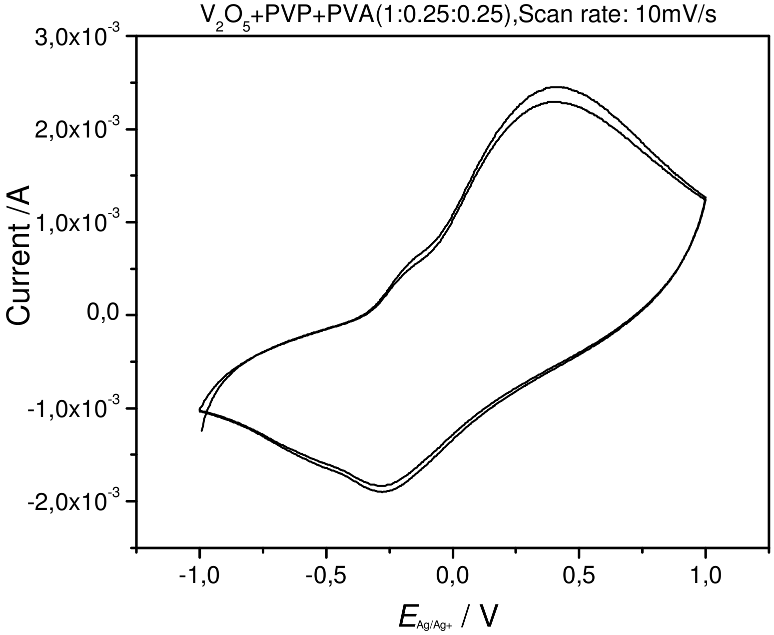

Figure 7. Cyclic voltammagram of reduced vanadium dioxide nanomaterials from V_2O_5 xerogel using 0. 5 M (PVP+ PVA) as a surfactant in non-aquous electrolyte (1 M $LiClO_4$ dissolved in propylene carbonate).

The cyclic voltammograms (CV) of (V_2O_5 + PVP + PVA) (1: 0.25:0.25) → VO_2 (B) nanowires and (V_2O_5 + PVA) (1: 0.5) → VO_2 (B) nanobelts are shown in Fig. 7 and 8. The CV of the working electrode made of nanowires shows broad anodic and cathodic peaks at 0.4 V and -0.25 V, respectively. These peaks are attributed to Li^+ extraction from the working electrode and intercalation into the working electrode [1]. The CV curves of the working electrode made of nanobelts also exhibits two broad cathodic peaks and one anodic peak at - 0.79 V, -0.6 V and + 0.44 V. The oxidation of V^{4+} →

V^{5+} happens at the anodic peak, and the reduction of $V^{5+} \rightarrow V^{4+}$ occurs at the cathodic peak. The CV curves of the working electrode made of nanowires show higher current density than the working electrode made of nanobelts due to higher conductivity of the polyblend(PVP+PVA) surfactant [20].

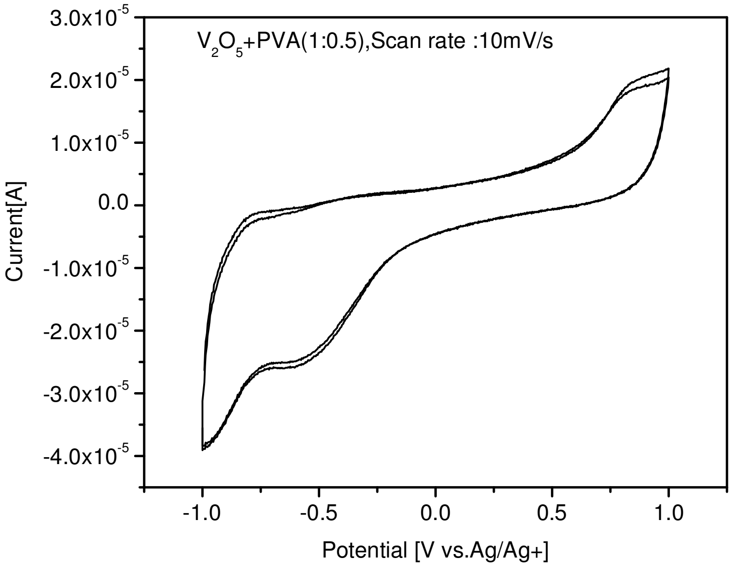

Figure 8. Cyclic voltammagram of reduced vanadium dioxide nanomaterials from V_2O_5 xerogel using 0. 5 M PVA as a surfactant in non-aquosis electrolyte (1M $LiClO_4$ dissolved in propylene carbonate).

4. CONCLUSIONS

Vanadium dioxide nanomaterials were synthesized through a simple hydrothermal process with the assistance of (PVP + PVA) and PVA. The conversion of $V^{4+} \rightarrow V^{5+}$ was confirmed from TGA and XRD analysis. The morphology of the nanowires (V_2O_5 + PVP + PVA) → VO_2 (B) and the nanobelts of (V_2O_5 + PVA) → VO_2 (B) have been confirmed by SEM micrographs. The cyclic voltammograms show the higher current density in the working electrode made of nanowires than that in the working electrode made of nanobelts.

ACKNOWLEDGEMENT

One of the authors (VS Reddy Channu) thank the Alexander von Humboldt Foundation for a fellowship. R. Kalluru and Q. Williams would like to thank JSU-Corning partnership.

References

1. Y. Wang, G. Cao, *Chem. Mater.* 18 (2006) 2787.
2. F. N. Crespilho, V. Zucolotto, O. N. Oliveira Jr., and F. C. Nart, *Int. J. Electrochem. Sci.,* 1 (2006) 194.
3. Ch. V. Subba Reddy, E. H. Walker Jr, S.A. Wicker Sr, Q.L. Williams, and R.R.Kalluru, *Current. App. Phys* 9 (2009) 1195.
4. F. Sediri , N. Gharbi, *Mater.Sci. Eng. B* 123 (2005) 136.
5. C. Tsang, A. Manthiram, *J. Electrochem.Soc.* 144 (1997) 520.
6. Ch. V. Subba Reddy, E. H. Walker Jr, S.A. Wicker Sr, Q.L. Williams, and R.R.Kalluru, *J. Electrochem. Soc*. 155 (2008) A599.
7. Ch. V. Subba Reddy, S.-I Mho, R. R. Kalluru and Q. L. Williams, *J. Power Sources*179 (2008) 854.
8. Y. Oka, T. Yao, N. Yamamoto, *J. Mater. Chem*. 1 (1991) 815.
9. F. Theobald, *J. Less-Common Met*. 53 (1977) 55.
10. F.J. Morin, *Phys. Rev. Lett.* 3 (1959) 34.
11. C. Tsang, A. Manthiram, *J. Electrochem. Soc*. 144 (1997) 520.
12. G.C. Li, K. Chao, H.R. Peng, K.Z. Chen, and Z.K. Zhang, *Inorg. Chem*. 46(2007) 5787.
13. G. Armstrong, J. Canales, A.R. Armstrong, and P. G. Bruce, *J. Power Sources* 178 (2008)723.
14. A. B. Moghaddam, T. Nazari, *Int. J. Electrochem. Sci.,* 3 (2008) 768.
15. C.-G. Wu, D. C. DeGroot, H. O. Marcy, J. L. Schindler, C. R. Kannewurf, Y.-J. Liu, W. Hirpo, and M. G. Kanatzidis, *Chem. Mater*.8(1996)1992.
16. W.Chen, Q. Xu, Y. S. Hu, Li- Q. Mai, and Q.- Y. Zhu*, J. Mater. Chem*.12(2002)1926.
17. Ch. V. Subba Reddy,S-I. Mho, R. R. Kalluru, and Q. L. Williams, *J. Power Sources* 179 (2008) 854.
18. F. Sediri , N. Gharbi, *Mater.Lett*. 63 (2009) 15.
19. Ch. V. Subba Reddy, K.-Il Park, S.-il Mho, In-H. Yeo, and Su-M. Park, *Bull. Korean Chem. Soc.* 29(2008)2061.
20. Ch.V. Subba Reddy, Xia Han, Q.-Y. Zhu, Li-Q. Mai, and W. Chen, *Microelectronic Engineering* 83 (2006) 281.